CHAPTER 3

Physical Aging of Membranes for Gas Separations

B.W. ROWE,[a,b] B.D. FREEMAN[a] AND D.R. PAUL*[a]

[a] Department of Chemical Engineering, Texas Materials Institute and Center for Energy and Environmental Resources, The University of Texas at Austin, Austin, Texas 78712, USA; [b] Polymers Division, National Institute of Standards and Technology, Gaithersburg, Maryland 20899, USA

3.1 Introduction

The polymers that comprise most high-performance gas separation membranes are amorphous, glassy materials.[1] These materials are selected based on their superior permeability and selectivity characteristics and their ability to form rigid structures that enable the development of self-supporting architectures, such as asymmetric hollow fibers.[2-4] The performance of gas separation membranes change with time due to the inherent non-equilibrium nature of glassy polymeric materials. As non-equilibrium materials, glassy polymers undergo physical aging, a spontaneous, but typically slow, evolution toward an equilibrium state.[5-7] However, the changes in material properties caused by physical aging are thermo-reversible, *i.e.* the changes can be reversed by heating the sample above the glass transition of the material. This important feature of physical aging separates the phenomenon from other factors that may influence behavior over time such as chemical aging, degradation, or contamination. Extensive studies on the influence of physical aging on glassy polymer behavior, *e.g.* mechanical properties, volume relaxation, and thermodynamic behavior, have been reported in the literature.[6-11] This chapter does not attempt to

summarize the entire field of physical aging, but will focus on the influence of aging on transport behavior of gas separation membranes and related material properties. Aging in glassy polymers causes permeability to decrease over time, requiring additional membrane area to treat a given process stream than originally needed based on initial performance. It is essential to understand the influence of physical aging on the performance of gas separation membranes when designing a membrane system to ensure satisfactory performance over long service periods.

Over the last several decades, research and development of selective ultra-thin membranes has gained tremendous momentum in an attempt to compete with alternative separation technologies, such as pressure swing adsorption and cryogenic distillation.[12–14] Because membrane permeance is inversely proportional to thickness, the development of ultra-thin active selective layers is required to maximize membrane productivity. The membrane support structure must also be optimized to minimize additional mass transfer resistance.[15] Commercially, the active separating layer of gas separation membranes can be on the order of 100 nm, with ongoing efforts to reduce this layer thickness to further increase membrane permeance. Ultra-thin selective layers are most commonly produced by coating a dilute polymer solution onto a microporous support to form composite membranes or by solution spinning techniques to produce asymmetric hollow fiber membranes.[4,16] Creating these thin film structures with limited defects is often the dominant challenge in membrane manufacturing, due to the extremely fragile nature of these ultra-thin films. A nearly defect-free film is imperative for high selectivity since even a small area fraction, on the order of 10^{-6}, can destroy the native gas selectivity of a material.[17]

The influence of film thickness and confinement on polymer behavior is an active research topic in polymer physics due to the importance of these factors in the development of a diverse range of technologies, including nanocomposite materials, microelectronics, coatings, and optics.[18–23] Although there is some debate regarding the influences of sample preparation and experimental conditions on the observed confinement effects, results indicate that the glass transition temperature of ultra-thin films can deviate substantially from bulk values.[24,25] These differences have been attributed to interfacial interactions between the polymer and substrate, or free surface.[26,27] Free standing films or films on non-attractive substrates exhibit decreasing glassy transition temperature (T_g) with film thickness, while strongly attractive substrates have been shown to increase the T_g of thin films. Furthermore, interfacial interactions have also been shown to influence aging behavior. For example, slower aging was observed for a 20 nm thick poly(methyl methacrylate) (PMMA) film on a silicon substrate as compared to 500 nm thick films; the reduced aging rate was attributed to restricted polymer chain mobility induced by attractive interfacial interactions.[28]

Thick film, *i.e.* bulk, samples are typically used when screening the transport properties of polymeric membrane materials, due to ease of handling and creation of defect-free films. Except for ultra-high free volume polymers such as

Table 3.1   Influence of film thickness and aging time on the transport properties of Matrimid[®31]

Matrimid[®]		Bulk (Literature values)	550 nm		18 nm	
			1 hr	1000 hr	1 hr	1000 hr
Permeability (Barrer)	O_2	2.12	3.35	1.95	1.68	0.57
	N_2	0.32	0.55	0.28	0.23	0.07
	CH_4	0.28	0.47	0.21	0.18	0.05
Selectivity	O_2/N_2	6.6	6.1	7.0	7.3	8.1
	N_2/CH_4	1.14	1.17	1.33	1.28	1.40

poly[1-(trimethyl-silyl)propyne] (PTMSP), which ages rapidly even in the bulk state, the transport properties of these thick glassy polymer films do not change dramatically with time due to physical aging.[29,30] Therefore, the reported permeabilities for a given polymer are typically within an acceptable range to allow comparison with other materials. However, when the glassy material is prepared in an ultra-thin film structure for industrial application, the polymer properties can differ significantly from bulk behavior. Table 3.1 illustrates the influence of film thickness and aging time on the gas transport properties of Matrimid a commercially available polyimide of interest for gas separation applications.[31]

Depending on film thickness, the initial permeability coefficients, measured at 1 h of aging, can be above or below the reported bulk values. After aging for approximately 1000 h, both thin films have lower permeability than the bulk. In the case of the 18 nm film, O_2 permeability decreased to ~25% of the bulk value after 1000 h of aging. These aging induced changes increase with penetrant size, as the larger molecules are more strongly affected by the loss of free volume that occurs during aging. This behavior causes pure gas selectivity to increase with aging, as seen in Table 3.1. Clearly, large deviations from bulk properties exist in ultra-thin films, and predicting the behavior of ultra-thin films from bulk measurements is only a rough approximation of the true behavior. These differences also highlight possible errors in the current methods used to estimate the selective layer thickness of asymmetric membranes using bulk permeability values. Furthermore, because these deviations from bulk behavior are not well understood, accurately predicting ultra-thin film behavior is particularly challenging. The goals of this chapter are to describe the recent discoveries related to accelerated aging in thin glassy films, highlight the advances in experimental techniques that have enabled these studies, and to discuss the current state of understanding of this phenomenon and the questions and opportunities that remain.

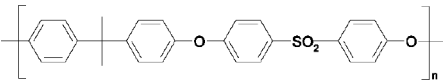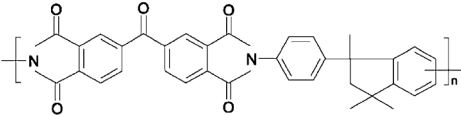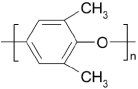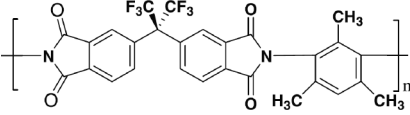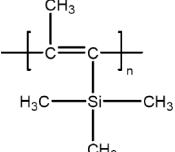## 3.2   Aging Behavior in Thin and Ultra-thin Films

The influence of thickness on aging behavior in gas separation membrane materials was first reported in the early 1990s; however, these aging effects may

have also been partially responsible for other time-dependent transport properties described in earlier reports.[32,33] For instance, although not originally considered as a controlling factor, physical aging may have contributed to the flux decline in asymmetric cellulose acetate membranes described by Baayens and Rosen.[34] Early reports on the influence of thickness on aging behavior compared bulk behavior to thin, complex membrane structures with ill-defined thermal histories and lacked accurate methods to determine film thickness. Rezac *et al.* reported the influence of aging time on the gas transport properties of thin and thick films of 6FDA-IPDA polyimide and tetramethyl-hexafluoropolycarbonate (TMHFPC).[32] While a 71 μm thick film of the 6FDA-IPDA polyimide maintained 98% of the initial nitrogen flux after 2 months of aging, the nitrogen flux through a thin film was reduced to 20% of the initial value after just 20 days of aging. The thickness of the thin film, which was formed on a porous ceramic support, was estimated to be $\sim$300 nm based on the initial permeance. This thickness was reportedly in fair agreement with values estimated from scanning electron microscopy (SEM) measurements and material balance calculations, *i.e.* thickness calculated based on the mass deposited and the polymer density. While the methods of thickness determination were approximate, the difference in the aging behavior of the thin film as compared to the bulk state was a clear indication that physical aging is influenced by film thickness. This work also showed the initial selectivity of the thin films started below the bulk value, but increased beyond the bulk value with aging time. Other studies showed similar influences of film thickness on aging behavior by comparing the time-dependent transport properties of thin-skinned asymmetric membranes and bulk films.[33,35]

Several experimental advances have enabled more systematic studies on the influence of film thickness on physical aging. Accurate film thickness measurements are essential in developing a fundamental understanding of these effects. Film thickness measurements of ceramic composite membranes using SEM were improved over previous techniques by comparing the back-scattered electron image, which only shows the higher atomic mass ceramic support layer, to the secondary electron image, which shows the support and film layers.[36] More recently, further improvement in thickness measurements were realized by using variable angle spectroscopic ellipsometry.[37] Ellipsometry measures the changes in elliptically polarized light that is reflected through a sample and can provide detailed information about thin films and surfaces. Although this technique has been applied in other fields, such as microelectronics, for some time, it has not been widely used to characterize gas separation membranes until recently. The application of this technique to the membrane field was a significant development in the ability to characterize thin films. In addition to very accurate thickness measurements, ellipsometry can provide optical properties, such as refractive index, that can be related to physical properties as another method for tracking physical aging.[38,39] The use of ellipsometry to study physical aging will be discussed in more detail later in the chapter. These improvements in thin film characterization also aided in the development of models for describing the aging response of thin glassy films.[40]

   Because the state of a glassy polymer and, therefore, its aging behavior, depend on the material's previous history in addition to the immediate experimental conditions, it is important to consider how materials are treated before testing in physical aging studies.[41,42] Unless otherwise specified, the results presented in this chapter were collected using films created by spin-coating that were subsequently heated above their glass transition temperature in a free standing state to erase any influence of previous history and then rapidly quenched to the aging temperature to define a reproducible starting time for the aging experiments. While these procedures may exaggerate the physical aging response by beginning with the material in a high free volume state, the consistency in the initial conditions is critical. Some discussion on the influences of different thermal histories and experimental procedures on physical aging in thin films will be given in Section 3.4. The chemical structures and bulk material properties of the polymers investigated in this chapter are given in Table 3.2.

Table 3.2 Bulk material properties

Polymer	T_g	P_{O_2}	P_{N_2}	P_{CH_4}	f_b
Polysulfone	186°C	1.4	0.24	0.29	0.144
Matrimid®	317°C	2.12	0.32	0.28	0.170
PPO	210°C	14.6	3.5	4.1	0.183
6FDA-DAM	372°C	55	17	15.1	0.19
PTMSP	>280°C	9000	6600	15000	0.29

Permeability values are given in Barrers: 1 Barrer $= 1 \times 10^{-10}$ [cm^3(STP) $\cdot$ cm/(cm$^2 \cdot$ s $\cdot$ cmHg)]
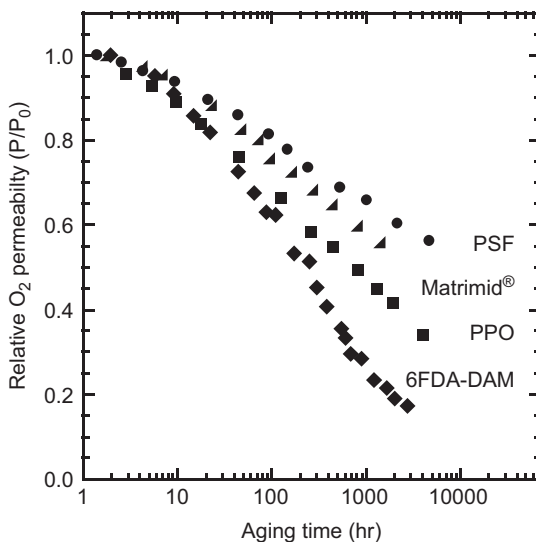PPO $=$ poly(2,6-dimethyl-1,4-phenylene oxide).
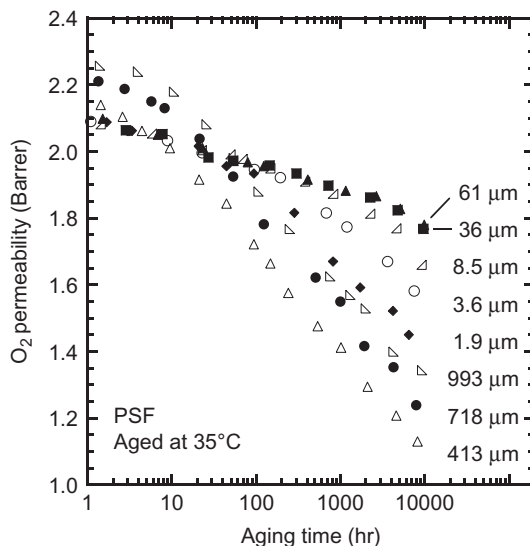
Figure 3.1   Influence of aging time on oxygen permeability coefficients in PSF films with thicknesses ranging from 61 μm (*i.e.* bulk) to 413 nm. Reproduced with permission of Elsevier.[43]

These polymers were chosen based on their importance in the gas separation field and because they are deep in the glassy state, *i.e.* far below T_g, at the temperatures of interest, which is approximately ambient for most applications.

The foundation for understanding how film thickness influences physical aging behavior begins with a systematic study on films across a broad thickness range with identical thermal histories. Figure 3.1 shows the influence of physical aging at 35 °C on the O_2 permeability coefficient of polysulfone (PSF) films with thicknesses (*l*) ranging from 61 μm to 413 nm.[43] While the relatively thick films, *i.e.* $l > 10$ μm, show only a modest decrease in permeability with aging time, the thin films, *i.e.* $l < 10$ μm, are strongly affected by physical aging.

As film thickness is reduced below 10 μm, the rate of O_2 permeability loss is greatly accelerated as compared to the thick film behavior. Additionally, the initial permeability of the thin films is higher than the bulk value; this result is presumed to be a result of the higher free volume state of the thin films after the rapid quench from above T_g. Surprisingly, while changes in the glass transition typically are not observed in films greater than ∼100 nm in thickness, physical aging can depend on dimensions that are on the order of microns. Similar to the results in Table 3.1, the pure gas selectivity through these films increased with physical aging as the material became more size selective due to the loss of free volume.

In addition to the results presented for PSF, analogous thickness-dependent aging behavior has been reported for other polymers.[36,43,44] Figure 3.2 compares the influence of aging time on the relative oxygen permeability of

Figure 3.2 Influence of aging time on relative oxygen permeability (based on permeability after 1 h of aging) in thin films of various polymers about 400 nm thick.

~400 nm thick films made from PSF, Matrimid, poly(2,6-dimethyl-1,4-phenylene oxide) (PPO), and 6FDA-DAM.

Again, the chemical structures and bulk properties, including fractional free volume, of these polymers are given in Table 3.2. Each of these materials shows a strong decrease in permeability with aging time when prepared as a thin film, and the magnitude of the aging-induced changes is highly dependent on the polymer structure.

In the case of PSF, the relative oxygen permeability decreased to 60% of the initial value after ~2000 h of aging, while the 6FDA-DAM polyimide retained less than 20% of its initial permeability after a similar aging period. The physical aging rate, as determined by the rate of relative permeability decline, of these polymers follows the same trend as the bulk fractional free volume, *i.e.* 6FDA-DAM > PPO > Matrimid > PSF. This trend could be expected, as the rate of physical aging is intimately related to the excess free volume in a material.[40] This comparison highlights the current need to study each material of interest to understand their behavior in thin film form. If connections between the bulk polymer properties and thin film behavior can be defined, better predictions of the influence of physical aging effects in thin films could be developed.

The extreme difficulty in creating and handling delicate thin films for gas permeation measurement early on limited the study of single-layer free standing films to a minimum thickness of 300–400 nm. Microscopic pinhole defects that destroy the selective of thin polymer membranes form with increasing frequency as film thickness is decreased.[45] To overcome this challenge, a
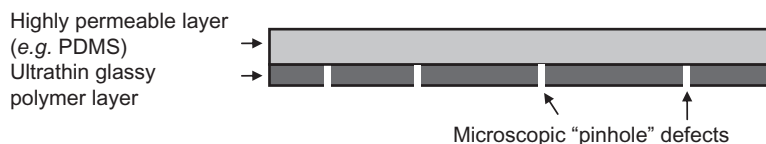
Figure 3.3 Diagram of film structure used by Rowe *et al.*, which enabled the study of gas permeability properties and physical aging behavior of ultra-thin glassy films. Reproduced with permission of Elsevier.[31]

coating technique, similar to that which initially facilitated the application of polymeric membranes to industrial application, was developed.[17,46] The thin glassy films were prepared using the spin coating methods described previously. Before removing the films from the silicon substrate, a thin layer of highly permeable poly(dimethylsiloxane) (PDMS) was coated directly on top of the thin glassy layer.

Figure 3.3 presents a schematic of the film structure utilized in this procedure. This rubbery layer effectively blocks convective flow through any pinhole defects but adds very little mass transfer resistance due to its high permeability.[47] Furthermore, the additional mass transfer resistance, which is constant over time for the rubbery layer, can be accounted for using a series resistance model:[15]

$$\frac{l_{\text{composite}}}{P_{\text{composite}}} = \frac{l_{\text{PDMS}}}{P_{\text{PDMS}}} + \frac{l_{\text{Glassy}}}{P_{\text{Glassy}}} \tag{3.1}$$

where l_{PDMS} and l_{Glassy} are the thicknesses of the PDMS and glassy polymer layers, respectively, and P_{PDMS} and P_{Glassy} are the permeability coefficients of the PDMS and glassy polymer, respectively. The total thickness of the composite film is $l_{\text{composite}} = l_{\text{PDMS}} + l_{\text{Glassy}}$, and the permeability of the composite film is $P_{\text{composite}}$. By measuring the thickness of each layer and knowing the permeability of PDMS, eqn (3.1) can be used to calculate the permeability of the glassy layer from measurements on the composite film.

The development of this coating technique has enabled the study of ultra-thin films with thicknesses that are of interest in gas separation membrane applications.[31] Figure 3.4(a) presents the influence of aging time on the oxygen permeability coefficients of Matrimid films down to 18 nm in thickness prepared with the coating technique. Note that the quoted film thickness is the thickness of the glassy layer.

The films were aged at 35 °C, which is 280 °C below the T_{g} of bulk Matrimid, in a dry environment between measurements. Despite being far below T_{g}, dramatic aging effects on gas permeability are evident in the ultra-thin films. The oxygen permeability decreased rapidly with aging time, to ∼50% of the initial value after 1000 h, in all films as the material evolved towards an equilibrium state. Interestingly, the initial permeability coefficient measured at 1 h of aging time decreases with film thickness in the ultra-thin films. This initially lower gas permeability is attributed to the rapid physical aging
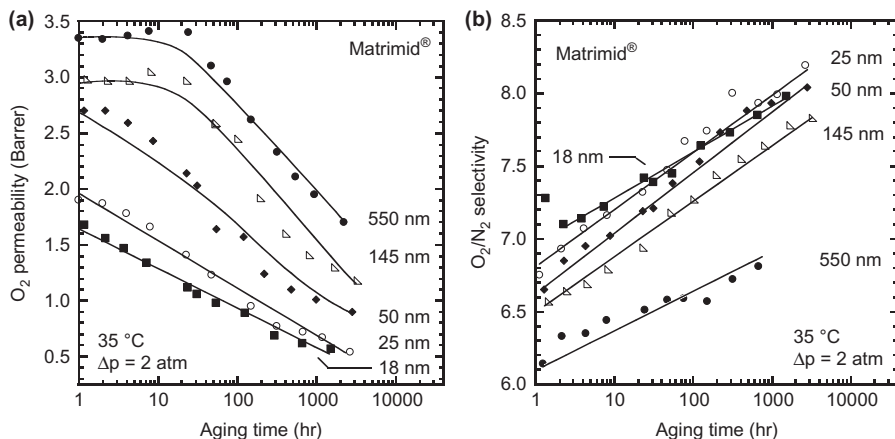
Figure 3.4   Influence of aging time on (a) oxygen permeability coefficients, and (b) O_2/N_2 pure gas selectivity in Matrimid® films with thicknesses ranging from 550 nm to 18 nm. Reproduced with permission of Elsevier.[31]

that occured during the first hour after the quench from above T_g; this time is required to prepare the sample for permeation testing using the current experimental techniques hence no data can be collected before 1 h. The notion that the initially measured permeabilities are different for the ultra-thin films is supported by recent modeling work, which will be described in Section 3.5.[31]

Figure 3.4(b) shows the O_2/N_2 pure gas selectivity as a function of aging time for the ultra-thin Matrimid films.[31] All films exhibit selectivities that are near or above the bulk selectivity value, 6.6, indicating the films are essentially defect free. The O_2/N_2 selectivity increases with physical aging, as expected; the reduction in free volume caused by physical aging makes the material more size selective by reducing the diffusion of the larger N_2 molecules more than that of smaller O_2 molecules. The increase in selectivity is fairly substantial; for instance, the O_2/N_2 selectivity of the 25 nm thick Matrimid film increases from an initial value of 6.75 to above 8.0 after 1000 h of aging. Additionally, selectivity increases with decreasing film thickness, consistent with the observation of decreasing permeability in thinner films described previously.

The ability to study ultra-thin films provides important guidelines for understanding the behavior of membranes used in gas separation applications. These films, with thicknesses similar to estimates of the skin layer in asymmetric hollow fibers, demonstrate that deviations from bulk behavior continue as film thickness is reduced. Of course, some questions remain regarding the behavior of more complex membrane structures and applications, *e.g.* how does the underlying structure of an asymmetric membrane affect aging, and how does exposure to high pressure multi-component feed streams with highly sorbing penetrants impact long-term performance? Due to the immense complexity of these issues, careful development of current and future experimental

techniques, in addition to improved theoretical models, is essential to fully understand how these factors influence thin film behavior.

3.3 Additional Experimental Methods used to Study Physical Aging

In addition to providing accurate measurements of film thickness, ellipsometry can also be used to determine the optical properties of thin films, *e.g.* refractive index, thus providing additional means to track the influence of aging on film properties.[38,39,48,49] The Lorentz–Lorenz equation provides a fundamental connection between refractive index and density:[50]

$$\frac{\bar{n}^2 - 1}{\bar{n}^2 + 2} = \frac{\rho N_{av}\alpha}{3M_0\varepsilon_0} \tag{3.2}$$

where ρ is the polymer density, N_{av} is Avogadro's number, α is the average polarizability of the polymer repeat unit, M_0 is the polymer repeat unit molecular weight, and ε_0 is the permittivity of free space. Only refractive index and density are anticipated to change with physical aging, reducing the Lorentz–Lorenz equation to:

$$L = \frac{\bar{n}^2 - 1}{\bar{n}^2 + 2} = \rho C \tag{3.3}$$

where L is defined as the Lorentz–Lorenz parameter. Because the specific refraction, C, is constant during physical aging, this relationship can be used to compare the relative density of materials during physical aging from measured refractive index values, even if the specific refraction is not known. Specific refraction parameters can be calculated from bulk values of density and refractive index, allowing density to be calculated as a function of aging time. Furthermore, density can be related to fractional free volume, FFV, as follows:

$$\text{FFV} = \frac{v - v_o}{v} = 1 - \rho v_o \tag{3.4}$$

where v is specific volume, (equivalent to $1/\rho$), and v_o is the occupied volume, which can be estimated by the Bondi method (*i.e.* $v_o = 1.3v_w$, where v_w is the van der Waals volume estimated using the group contribution method).[51] This method to determine free volume can be used to track free volume changes over time and aid in the development of theoretical physical aging models.

Figure 3.5 presents the relative density, calculated using eqn (3.3), of 400 nm thick films made from four different polymers as a function of aging time at 35 °C.[38,49] The results from these ellipsometry studies directly show that these thin films densify during the physical aging process. The rate of densification depends strongly on the polymer type. Again, the rate of aging follows the same
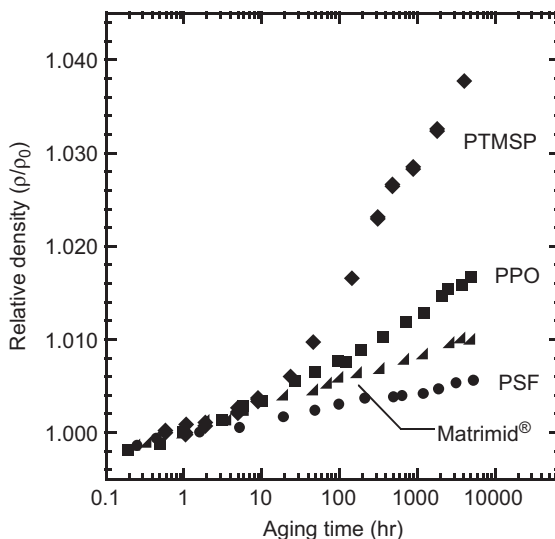
Figure 3.5   Influence of aging time on relative density (calculated using the Lorentz–
Lorenz equation and based on density after 1 h of aging) in thin films of
various polymers about 400 nm thick.

order as the fractional free volume, listed in Table 3.2, *i.e.* poly(1-trimethylsilyl-
1-propyne) (PTMSP) > PPO > Matrimid > PSF. The ultra-high free volume
polymer, PTMSP, shows significantly faster physical aging than the other
glassy materials. The density of PTMSP increases by nearly 4% from its initial
value after several thousand hours of aging, while the other materials show
density increases of 0.5–1.5%. These films were all approximately 400 nm thick
and prepared by spin coating onto silicon wafer supports. Three of the poly-
mers, PSF, PPO, and Matrimid where heated above their T_g prior to the aging
studies; however, PTMSP decomposes before reaching its glass transition.[52]
Therefore, the PTMSP film did not begin the aging experiment from a freshly
quenched state and was heated to 180 for 90 min to remove any residual solvent
prior to the aging study; both of these factors would presumably retard the
aging response of a material in comparison to the freshly quenched state.
Considering these factors, PTMSP might be expected to age even faster than
represented by these results if the experiments were conducted using a PTMSP
sample with higher initial free volume.

In addition to characterizing the influence of aging on density, results from
aging studies using ellipsometry have also been shown to correlate well with gas
permeability measurements.[40,44] Direct comparison of volumetric aging rates
determined by ellipsometry to rates of permeability decline shows a strong
correlation to the properties probed using these two different techniques.

Another experimental technique that has been useful in studying physical
aging of glassy polymers is positron annihilation lifetime spectroscopy

(PALS).[9,10,53,54] PALS provides unique information about the free volume properties of amorphous materials by measuring the lifetime of injected positrons.[55,56] The lifetime of ortho-positronium (o-Ps), τ_3, can be related to the size of free volume elements in the sample by assuming a spherical cavity shape and using the relationship given in eqn (3.5):

$$\tau_3 = \frac{1}{2}\left[1 - \frac{r}{r + \Delta r} + \frac{1}{2\pi}\sin\left(\frac{2\pi r}{r + \Delta r}\right)\right]^{-1} \qquad (3.5)$$

where r is the cavity radius and Δr is the e^- layer thickness (1.656 Å).[57,58] Furthermore, the relative number of positrons that annihilate as o-Ps, the o-Ps intensity (I_3), is related to the concentration of free volume elements in a material.

While PALS has been used in numerous studies to investigate physical aging of polymeric membrane materials, the standard technique is limited to studying bulk samples because of the high energy of the source positrons.[56] By combining positron annihilation lifetime spectroscopy with a slow mono-energetic positron beam, thin films of interest for gas separation applications can be studied. Additionally, the energy, and therefore, implantation depth, of the positron beam can be controlled, allowing the free volume properties of a film to be studied as a function of distance from the free surface.[59,60] The ability to probe the free volume property profile as a function of aging time provides vital information for developing and validating mechanistic physical aging models. In addition to aging studies on dense thin films, this variable energy PALS technique has been used to study asymmetric thin film structures.[61–63] The ability to study samples in a wet condition, during what would typically be a high vacuum experiment, was recently achieved by using a plasma-enhanced chemical vapor deposition technique to seal the sample prior to study.[63] These unique experimental techniques provide important information for understanding the influences of film thickness and interfacial interactions on membrane behavior by probing material properties that are difficult or impossible to measure by other means.

Figure 3.6 shows the average o-Ps lifetime, τ_3, as a function of mean implantation depth for thin PSF films ($l = 450$ nm) after aging for various times on silicon wafer supports.[64] Each lifetime profile represents a different PSF film that was aged at 35 °C for the time indicated in the figure. The o-Ps lifetime decreases with physical aging at all implantation depths. The decrease in τ_3 corresponds to a decrease in the average free volume element size with aging, which is expected as the material approaches a more dense, equilibrium state. Interestingly, the average free volume element size, as related to τ_3, is reduced near the film surface as compared to the center of the film. This intriguing result is thought to be caused by the initially rapid physical aging that occurs near the film surface, thus reducing τ_3 near the surface as compared to the remainder of the film. While the τ_3 profile is not symmetric about the center of the film, the o-Ps lifetime is also lower near the silicon substrate as compared to the film center. This lack of symmetry in the apparent τ_3 profile may be related to
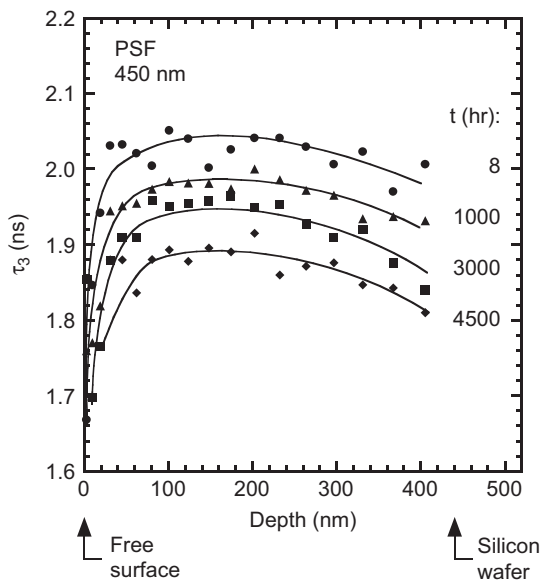
Figure 3.6   Influence of positron implantation depth and physical aging on *o*-Ps
                 lifetime in thin PSF films. Lines are provided to guide the eye. Reproduced
                 with permission of Elsevier.[64]

the change in implantation depth probability with beam energy, *i.e.* the
depth–sensitivity of the positron beam decreases as the implantation depth
increases.[65] It should be noted that while these films were studied on a silicon
support, they were prepared and aged in the free standing state to allow
comparison with results from gas permeability studies. Furthermore, no
influence of the silicon support on aging behavior was detected using this
technique by studying films that had been aged with and without the silicon
support.[64]

The variable energy PALS measurements also gave information on the *o*-Ps
intensity, which can be related to the concentration of free volume elements in a
sample, as a function of aging time and implantation depth; however, no
influence of aging on the *o*-Ps intensity profile was detected.[64] The constant
value of I_3 with aging time suggests that the loss of free volume in these thin
films with aging was caused solely by shrinking of the free volume elements.
This result indicates that the accelerated aging in these thin films, as compared
to the bulk material, is caused by a thickness-dependent lattice contraction type
mechanism that allows the material near the surface to age more rapidly than
the bulk, thus resulting in the lower free volume element sizes near the film
surface. Although diffusion based models can often describe thin film aging
behavior, this type of mechanism would suggest that physical aging causes
a reduction in the number of elements, and no significant change in the con-
centration of free volume elements was measured using this technique.

The depth profile of free volume properties measured using variable energy PALS provides an opportunity to investigate the aging behavior as a function of depth from the free surface. The average *o*-Ps lifetime across a specific section of the film, $\bar{\tau}_3$ can be calculated by:

$$\bar{\tau}_3 = \frac{\sum(\tau_{3i} \times \Delta l_i)}{l} \tag{3.6}$$

where τ_{3i} is the *o*-Ps lifetime across distance Δl_i and *l* is the total thickness of the film section of interest. Figure 3.7 illustrates the influence of physical aging on the average *o*-Ps lifetime across three different sections of the PSF film, *i.e.* 50 nm from the free surface, 125 nm from the free surface, and the entire 450 nm film.

The sections of interest are highlighted in the inset of Figure 3.7. Initially, at 8 h of aging, the average *o*-Ps lifetime decreases with decreasing penetration depth. This result is attributed to the rapid aging that occurs in the near-surface region of the film during the first 8 h of aging, and is consistent with observations from the gas permeability studies, *i.e.* the initial gas permeability decreased with decreasing film thickness. Due to the time required to measure the positron lifetime spectra, the first measurements were conducted after 8 h of aging to minimize any changes that may occur over the experimental time scale due to physical aging. The average *o*-Ps lifetime decreased similarly in each section of the film from 8 to 3000 h of aging.
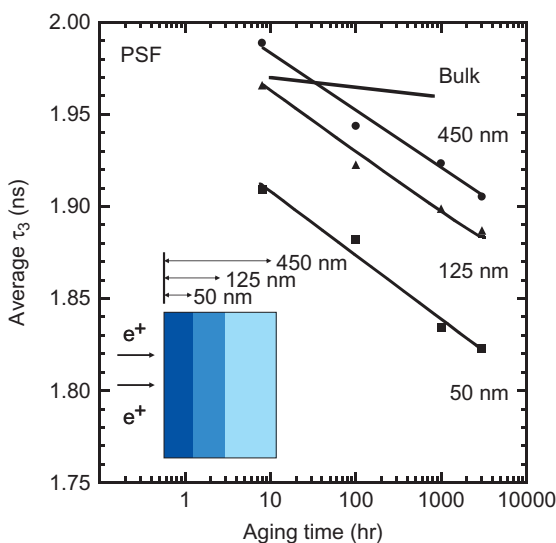
Figure 3.7 Influence of physical aging on the *o*-Ps lifetime averaged across different penetration depths of a 450 nm thick PSF film. Bulk aging behavior included for comparison. Inset schematic shows the film regions of interest. Lines are provided to guide the eye. Reproduced with permission of Elsevier.[64]

As seen from these results, variable energy PALS can provide useful information in determining the influences of film thickness and interfacial interactions on physical aging behavior. Furthermore, free volume properties, calculated from the variable energy PALS results, were used to estimate the gas transport behavior of the different sections of the PSF film.[64] Good agreement between the PALS-estimated permeabilities and experimentally measured values highlights the connection between changes in free volume and transport properties caused by physical aging.

Numerous other experimental techniques have been used to investigate the properties and behavior of thin polymeric films, including broadband dielectric spectroscopy, fluorescence spectroscopy, X-ray and neutron reflectivity, and more.[24,66–68] While most of these techniques have not been utilized to investigate the physical aging behavior of gas separation membrane materials, they offer unique perspectives into thin film behavior. Fluorescence spectroscopy has been used to study physical aging of thin polymeric films of PMMA and polystyrene.[28] Furthermore, clever experimental design and sample preparation techniques also enabled the study of polymer properties at specific locations relative to film interfaces using fluorescence spectroscopy.[21] Continued development of experimental techniques and application to gas separation membrane materials will certainly add to the understanding of ultra-thin film behavior.

3.4   Influence of Previous History and Experimental Conditions on Aging

The techniques used to create gas separation membranes, *e.g.* choice of casting solvent, drying treatment, *etc.*, can strongly affect their performance. For melt-processed films, or films heated above the glass transition during preparation, the rate at which the material is cooled from above T_g also has a significant influence on the final physical properties.[69–71] For example, rapidly quenched glasses exhibit accelerated aging when compared to slow-cooled samples, due to their initially higher free volume state.[72] After the polymer vitrifies, *i.e.* enters the glassy state, various treatments can alter its thermodynamic state, such as, mechanical stresses, thermal annealing, and exposure to highly sorbing penetrants.[41,73–75] For instance, in bulk glassy polymers, exposure to high pressure CO_2 causes the glassy polymer to swell, and after removal of the CO_2, the polymer structure does not immediately return to its initial state, effectively reducing its density.[75,76] While the effects of various conditioning treatments on polymer properties have been demonstrated in bulk materials, it is not well understood how thin films would respond to similar treatments.

Because glassy polymer properties depend strongly on previous history and experimental conditions, studies on these materials require samples with well-defined histories and consistent methodologies for meaningful comparisons. In the aging studies described previously in this chapter, a controlled quench from above the glass transition was used to define the experimental starting time; however, actual application of these materials in gas separation

membranes can involve very complex histories. The ultra-thin glassy films used in gas separation membranes are often products of elaborate phase inversion processes; additionally, the membranes may be subjected to further treatment steps and long periods of storage before use in the field. Moreover, while the earlier studies focused on films that were aged in a controlled, dry environment and exposed to only permanent gases, *i.e.* O_2, N_2, He, *etc.*, commercial gas separation membranes are exposed to a wide variety of process gases and contaminants that can strongly affect their performance. Because of these complexities, it is important to understand how aging behavior depends on a material's previous history and experimental conditions to accurately predict the long-term performance of practical gas separation membranes.

In an effort to understand how the initial state of a thin film affects its aging behavior, PSF samples were annealed for times ranging from 2 to 160 h at 170 °C, ∼15 °C below its T_g, prior to gas permeability and aging measurements.[77] Figure 3.8 shows the O_2 permeability coefficients as a function of aging time for the 125 nm thick PSF films that were annealed at 170 °C for the specified times after quenching from above T_g.

The base case represents a sample of identical thickness that began aging at 35 °C immediately following the quench from above T_g. As in the previous studies, all films were aged at 35 °C in a dry environment between measurements. The initial O_2 permeability decreased with longer annealing times at 170 °C, as expected, due to the influence of aging the material at the elevated temperature. While the aging responses were similar between all PSF films, the
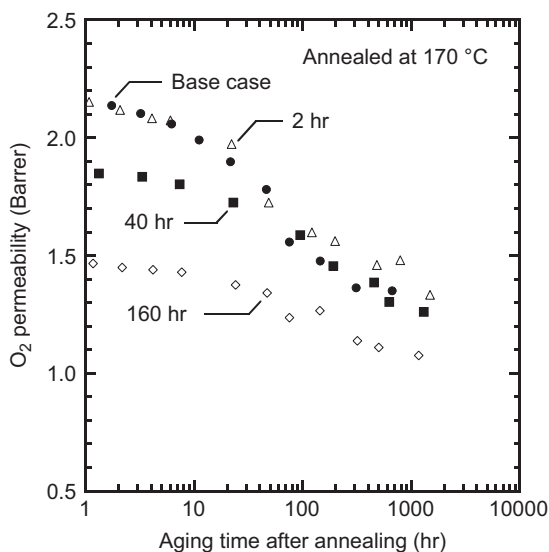

Figure 3.8 Influence of aging time at 35 °C on O_2 permeability coefficients in thin PSF films annealed for specified time at 170 °C after a quench from above T_g. Reproduced with permission of Elsevier.[77]

magnitude of aging induced permeability changes decreased with annealing time at 170 °C. The slower apparent aging rate in the annealed samples is consistent with the loss in driving force toward equilibrium, *i.e.* the annealed films had less excess free volume than the base case material. These observed trends in the aging behavior of annealed samples were well described by recent modeling efforts that account for the material's altered initial free volume state while using the same material properties as the base case.[77] Analogous behavior was seen for other probe gases, including N_2 and CH_4.

In addition to the conditioning effects that exposure to high pressure CO_2 has on glassy polymer properties, exposure to low pressures of highly sorbing gas can also affect membrane performance and aging behavior.[78,79] Figure 3.9 displays the influence of intermittent exposure to low pressure CO_2 (2 bar) on the aging behavior of thin 6FDA-DAM films, as tracked by methane permeability.[78]

The periods of exposure to low pressure CO_2 were spaced every 10–20 h or longer, and exposure times were about 30 min each. Surprisingly, with exposure pressure to only 2 bar of CO_2 over times that were short in comparison with the aging time scales, significant effects on the aging behavior are apparent. Both 6FDA-DAM films show decreasing CH_4 permeability with aging time; however, the influence of aging is notably reduced in the case of the film that had been intermittently exposed to CO_2. The impact of this exposure protocol on permeability changes with aging also depends on the size of the probe molecule.
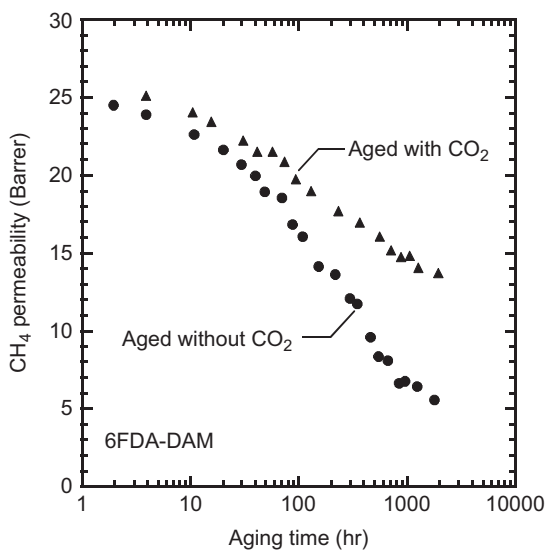
Figure 3.9 Influence of exposure to CO_2 during physical aging on the aging response in 6FDA-DAM as tracked by methane permeability. Throughout the aging process, the film was periodically exposed to CO_2 for short periods (~ 10 min) at 2 atm pressure. Reproduced with permission of Elsevier.[78]

While CO_2 exposure strongly affected the aging behavior of 6FDA-DAM as tracked by N_2 and CH_4 permeability, it did not significantly influence the He or O_2 permeability responses. Because the exposure to CO_2 slowed the permeability decline of larger molecules more than that of smaller molecules, the pure gas selectivity of these films actually decreased with aging time.[78] The strong influence that CO_2 exposure has on the aging behavior of thin films highlights the importance of understanding its role in the behavior of gas separation membranes.

While the properties of bulk membrane materials are typically only affected by exposure to CO_2 at relatively high pressures (tens of bars), thin film behavior can be affected at much lower pressures with exaggerated or even qualitatively different responses than those seen in thick films. This difference in response to CO_2 exposure is another example of the deviations from bulk behavior that manifest in thin glassy films. Because of the complex, and sometimes overlapping, effects of physical aging, plasticization, and penetrant-induced structural relaxation on thin film behavior, carefully designed experiments are required to identify the mechanisms responsible for the observed changes. Some evidence in the literature suggests thin films are more easily plasticized than bulk materials, and current research efforts show that this behavior is also dependent on sample history.[80–82] As might be expected, thin films display more pronounced hysteresis than thick films exposed to the same experimental cycle.[82] The impact that CO_2 has on the behavior of thin gas separation membranes indicates that these systems will also be strongly affected by other highly sorbing species that may exist in practical processing streams.

3.5 Modeling Physical Aging Behavior

While several models have been proposed to describe accelerated aging in thin polymer films, including the diffusion of free volume and thickness-dependent lattice contraction, efforts to more fully understand the mechanisms responsible for this behavior are ongoing. Physical aging models are typically characterized by a relaxation time, which represents chain mobility, and a measure of the current deviation from the predicted equilibrium, which represents the driving force. Models commonly used to describe physical aging, or isothermal relaxation, have foundations in work by Tool, Kovacs and others.[83–85] These models typically follow the form:

$$\text{aging rate} = \frac{\mathrm{d}v}{\mathrm{d}t} = \frac{-(v - v_\infty)}{\tau(v, T_g - T)} \tag{3.7}$$

where v and v_∞ are the polymer specific volumes at time t and at equilibrium, respectively, T is the system temperature, and τ is a characteristic relaxation time. A diffusion-based model developed by Curro *et al.*, based on Fick's second law, estimates free volume mobility using the well-known Doolittle relationship and implicitly includes the dependence of thickness on aging.[86] A related model with an alternative method for calculating vacancy diffusion,

termed the empirically derived vacancy diffusion model, has been developed more recently.[87] Although these models have been used to describe a variety of aging data in a phenomenological manner, the mechanisms that cause accelerated aging remain unclear.[40,88]

A straightforward model to describe aging in ultra-thin films was recently proposed based on the self-retarding aging model developed by Struik, which described the variation in many physical properties (*e.g.* specific volume, impact strength, and creep compliance) of bulk glassy polymers with aging.[6] According to this model, the change in free volume with aging time can be described by:

$$\frac{d\Delta f}{dt} = \frac{-\Delta f}{\tau} = \frac{-\Delta f}{\tau_\infty \exp(-\gamma \Delta f)} \tag{3.8}$$

where Δf is the excess fractional free volume (*i.e.* $f(t) - f_e$, where f_e is the equilibrium free volume), τ is the relaxation time at time t, τ_∞ is the relaxation time at equilibrium, and γ is a material constant characterizing the sensitivity of relaxation time to excess fractional free volume. Fractional free volume, FFV or f, can be calculated using eqn (3.4). While this model was validated using data from bulk polymers, where thickness effects on physical aging are not observed, τ_∞ can be allowed to depend on film thickness as a means to capture thickness-dependent aging behavior.

The fractional free volume, f, calculated as a function of aging time using the Struik model can then be used in the following correlation to give gas permeability:

$$P = Ae^{-B/f} \tag{3.9}$$

where A and B are constants based on bulk membrane permeability measurements.[89] The combination of this correlation between permeability and free volume and the thickness-dependent Struik model has been referred to as the modified Struik model.[31]

Figure 3.10(a) compares the experimentally measured permeability coefficients to predictions based on the modified Struik model for PSF films from 465 to 20 nm thick.[31] The model accurately captures the aging response when τ_∞ is allowed to change with films thickness; the γ value used was 350. The aging behavior of the ultra-thin PSF films is similar to that of the Matrimid® material shown in Figure 3.4(a), which is also well represented by the modified Struik model.[31] The τ_∞ values used in the model are shown in Figure 3.10(b) as a function of film thickness. The strong decrease of τ_∞ with film thickness below about 100 nm suggests that these ultra-thin films age more rapidly than thick films due to an enhanced rate of relaxation. Interestingly, the τ_∞ values show a similar sensitivity to film thickness as the glass transition temperature measured using ellipsometry as reported by Kim *et al.*, suggesting that the mechanisms that cause an apparent reduction in T_g are related to the accelerated aging of ultra-thin films.[90]
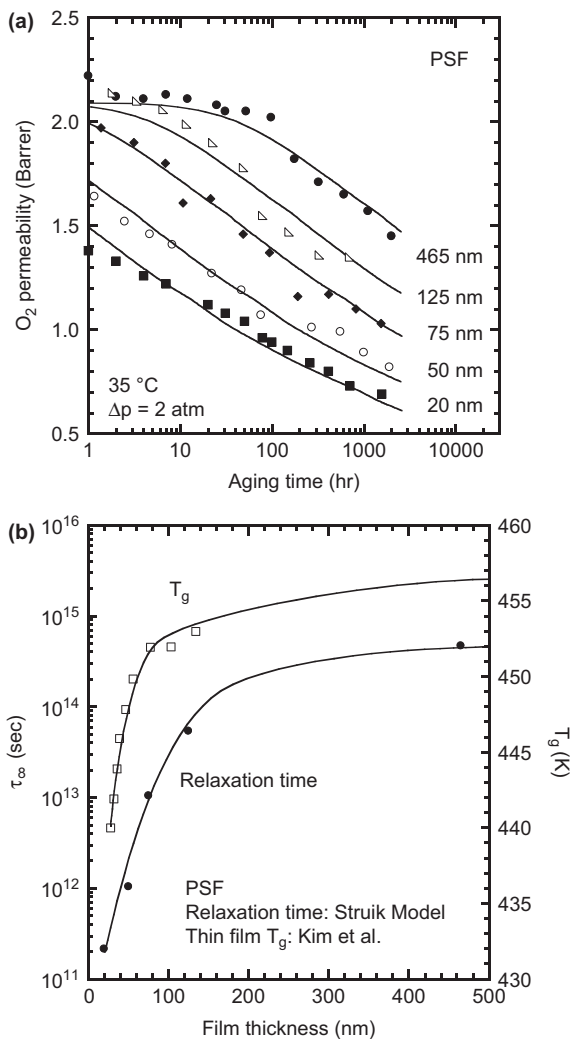
Figure 3.10 Influence of film thickness on physical aging and relaxation rates. (a) Effect of aging time on oxygen permeability coefficients in PSF films ranging from 465 nm to 20 nm in thickness. Lines were generated from the modified Struik model. (b) Dependence of τ_∞ and T_g, from Kim *et al.*, on PSF film thickness. Lines drawn to guide the eye in Figure 3.8(b). Reproduced with permission of Elsevier.[31]

The modified Struik model, as applied to these ultra-thin PSF films, used the same initial conditions for each film, *i.e.* at a short, finite time following the quench from above T_g, permeability was independent of film thickness. Figure 3.11 presents the model predicted O_2 permeability coefficients for the PSF films, including aging times $\ll 1$ h.
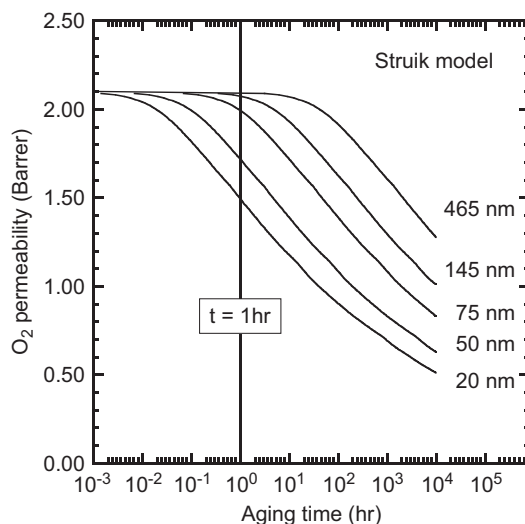
Figure 3.11   Influence of aging time and film thickness on the predicted oxygen permeability behavior of the PSF films studied based on the modified Struik model. Reproduced with permission of Elsevier.[31]

The vertical line drawn at 1 h of aging time highlights why the initial gas transport measurements show decreasing permeability as film thickness is reduced. The applied model is also consistent with the results of the variable energy PALS study discussed previously.[64] It was suggested that the smaller free volume elements near the film surface resulted from enhanced mobility in the near-surface region over the bulk. While, standard aging models, which do not account for thickness-dependent behavior, might suggest that the smaller free volume elements near the surface would age more slowly (due to decreased driving force) as compared to larger vacancies in the film center, the enhanced mobility of the near-surface region suggested by the model, counterbalances the reduced driving force, resulting in more rapid aging.

3.6   Concluding Remarks

Understanding the influences of film thickness and confinement on the physical aging behavior of glassy materials utilized in gas separation membranes is essential for predicting their long-term performance. Since physical aging was first recognized to depend on film thickness, multiple experimental advances have enabled more accurate characterization of these materials and their behavior. Techniques related to creating the defect-free films needed for gas transport measurements, precisely measuring film thickness, and handling the delicate structures have all contributed to the improved understanding of thin membrane behavior.

The results presented in this chapter suggest that the accelerated aging of ultra-thin films of gas separation membrane materials is caused by an enhanced mobility near the film surface that allows the polymer to relax towards an equilibrium state more rapidly than bulk samples. This deviation from thick film behavior is also strongly dependent on the polymer structure, complicating efforts to predict thin film behavior from bulk properties. Although some modeling efforts capture thickness dependent properties, estimating thin film behavior from bulk measurements only provides a first-order approximation.

The majority of systematic aging studies have focused on tracking material properties immediately following a quench from above T_g to define a consistent time zero and equivalent thermal history for different samples. The application of this technique is complicated for composite or asymmetric materials that may collapse or undergo macroscopic changes at elevated temperatures. Additionally, some high-performance materials have glass transition temperatures that are above the onset of decomposition, *e.g.* PTMSP, polymers of intrinsic microporosity, and some thermally rearranged polymers.[91–93] These complex structures and materials require alternative methods to reset or at least standardize their thermal history and create a meaningful starting point for aging studies. Physical aging studies on PTMSP have used a swelling non-solvent, *e.g.* methanol, to minimize aging effects prior to measurements and in efforts to create similar initial conditions between different samples.[94] These challenges also provide opportunities to better understand the influence of processing conditions and previous history on subsequent aging behavior in membrane materials.

Significant changes in physical properties occur over shorter times as the time scale for structural relaxation decreases with decreasing membrane thickness. This behavior is highlighted by the gas permeability results that show decreasing permeability coefficients with decreasing thickness in the ultra-thin films after just 1 h of aging.[31] Rapid, or *in situ*, experimental measurements are needed to accurately characterize the state of ultra-thin membranes immediately following a quench from above T_g, and to test the assumption that this method provides a consistent initial state for films across a wide thickness range.

Some of the initial investigations that reported thickness-dependent aging behavior were conducted using asymmetric hollow fiber membranes with complex histories and structures. With goals to better understand the role of film thickness on aging, research efforts shifted focus to dense isotropic membranes with well defined histories and well characterized thickness. While these studies provide valuable information regarding the influence of film thickness and the free surface on physical aging, the behavior of these isotropic membranes may still be different than that of the complex structures used in commercially produced membranes. For example, the rapid quench from above T_g in the free standing film studies accentuates the membrane's initial free volume state, and, subsequently, accelerates its aging behavior. Unraveling the influences of the film formation conditions and the connection to the underlying asymmetric structure on physical aging is perhaps the most

significant challenge in understanding the long term performance of gas separation membranes. Additionally, the exposure to condensable gases and vapors that may be present in process feed streams can strongly influence the aging behavior of ultra-thin membrane materials, even at low pressures. If the influences that these factors have on aging are better understood with new advances in experimental techniques, more accurate long-term performance predictions can be made, and perhaps ways to slow or arrest physical aging can be identified.

References

1. R. W. Baker, *Ind. Eng. Chem. Res.*, 2002, **41**, 1393.
2. L. M. Robeson, *J. Membr. Sci.*, 1991, **62**, 165.
3. L. M. Robeson, *J. Membr. Sci.*, 2008, **320**, 390.
4. D. W. Wallace, C. Staudt-Bickel and W. J. Koros, *J. Membr. Sci.*, 2006, **278**, 92.
5. C. A. Angell, K. L. Ngai, G. B. McKenna, P. F. McMillan and S. W. Martin, *J. Appl. Phys.*, 2000, **88**, 3113.
6. L. C. E. Struik, *Physical Aging in Amorphous Polymers and Other Materials*, Elsevier, Amsterdam, 1978.
7. J. M. Hutchinson, *Prog. Polym. Sci.*, 1995, **20**, 703.
8. A. R. Berens and I. M. Hodge, *Polym. Eng. Sci.*, 1984, **24**, 1123.
9. Y. Kobayashi, W. Zheng, E. F. Meyer, J. McGervey, A. Jamieson and R. Simha., *Macromolecules*, 1989, **22**, 2302.
10. A. J. Hill, K. J. Heater and C. M. Agrawal, *J. Polym. Sci. Part B: Polym. Phys.*, 1990, **28**, 387.
11. I. M. Hodge, *Science*, 1995, **267**, 1945.
12. R. W. Baker, *Membrane Technology and Applications*, John Wiley and Sons, Chichester, 2004.
13. A. S. Stern, *J. Membr. Sci.*, 1994, **94**, 1.
14. W. J. Koros and G. K. Fleming, *J. Membr. Sci.*, 1993, **83**, 1.
15. J. M. S. Henis and M. K. Tripodi, *J. Membr. Sci.*, 1981, **8**, 233.
16. I. Pinnau, J. G. Wijmans, I. Blume, T. Kuroda and K. V. Peinemann, *J. Membr. Sci.*, 1988, **37**, 81.
17. J. M. S. Henis and M. K. Tripodi, *Science*, 1983, **220**, 11.
18. J. L. Keddie, R. A. L. Jones and R. A. Cory, *Europhys. Lett.*, 1994, **27**, 59.
19. B. Frank, A. P. Gast, T. P. Russell, H. R. Brown and C. Hawker, *Macromolecules*, 1996, **29**, 6531.
20. C. W. Frank, V. Rao, M. M. Despotopoulou, R. F. W. Pease, W. D. Hinsberg, R. D. Miller and J. F. Rabolt, *Science*, 1996, **273**, 912.
21. C. J. Ellison and J. M. Torkelson, *Nat. Mater.*, 2003, **2**, 695.
22. R. Ruiz, H. M. Kang, F. A. Detcheverry, E. Dobisz, D. S. Kercher, T. R. Albrecht, J. J. de Pablo and P. F. Nealey, *Science*, 2008, **321**, 936.
23. J. A. Forrest and K. Dalnoki-Veress, *Adv. Colloid Interface Sci.*, 2001, **94**, 167.

24. R. Inoue, T. Kanaya, K. Nishida, I. Tsukushi, M. T. F. Telling, B. J. Gabrys, M. Tyagi, C. Soles and W. I. Wu, *Phys. Rev. E*, 2009, **80**, 031802.

25. M. Y. Efremov, A. V. Kiyanova and P. F. Nealey, *Macromolecules*, 2008, **41**, 5978.

26. C. J. Ellison, S. D. Kim, D. B. Hall and J. M. Torkelson, *Eur. Phys. J. E*, 2002, **V8**, 155.

27. C. B. Roth and J. R. Dutcher, in *Soft Materials: Structure and Dynamics,* ed. J. R. Dutcher and A. G. Marangoni, Marcel Dekker, New York, 2005, pp. 1–38.

28. R. D. Priestley, L. J. Broadbelt and J. M. Torkelson, *Macromolecules*, 2005, **38**, 654.

29. T. Masuda, E. Isobe, T. Higashimura and K. Takada, *J. Am. Chem. Soc.*, 1983, **105**, 7473.

30. S. D. Kelman, S. Matteucci, C. W. Bielawski and B. D. Freeman, *Polymer*, 2007, **48**, 6881.

31. B. W. Rowe, B. D. Freeman and D. R. Paul, *Polymer*, 2009, **50**, 5565.

32. M. E. Rezac, P. H. Pfromm, L. M. Costello and W. J. Koros, *Ind. Eng. Chem. Res.*, 1993, **32**, 1921.

33. P. H. Pfromm and W. J. Koros, *Polymer*, 1995, **36**, 2379.

34. L. Baayens and S. L. Rosen, *J. Appl. Polym. Sci.*, 1972, **16**, 663.

35. P. H. Pfromm and W. J. Koros, *Polym. Mater. Sci. Eng.*, 1994, **71**, 401.

36. M. S. McCaig and D. R. Paul, *Polymer*, 2000, **41**, 629.

37. Y. Huang and D. R. Paul, *J. Membr. Sci.*, 2004, **244**, 167.

38. Y. Huang and D. R. Paul, *Macromolecules*, 2006, **39**, 1554.

39. J. H. Kim, W. J. Koros and D. R. Paul, *Polymer*, 2006, **47**, 3104.

40. Y. Huang, X. Wang and D. R. Paul, *J. Membr. Sci.*, 2006, **277**, 219.

41. A. R. Berens and I. M. Hodge, *Macromolecules*, 1982, **15**, 756.

42. I. M. Hodge and A. R. Berens, *Macromolecules*, 1982, **15**, 762.

43. Y. Huang and D. R. Paul, *Polymer*, 2004, **45**, 8377.

44. J. H. Kim, W. J. Koros and D. R. Paul, *Polymer*, 2006, **47**, 3094.

45. G. Reiter, G. Reiter, M. Hamieh, P. Damman, S. Sclavons, S. Gabriele, T. Vilmin and E. Raphaël, *Nat. Mater.*, 2005, **4**, 754.

46. J. M. S. Henis and M. K. Tripodi, *Sep. Sci. Technol.*, 1980, **15**, 1059.

47. T. C. Merkel, V. I. Bondar, K. Nagai, B. D. Freeman and I. Pinnau, *J. Polym. Sci. Part B: Polym. Phys.*, 2000, **38**, 415.

48. H. Richardson, I. Lopez-Garcia, M. Sferrazza and J. L. Keddie, *Phys. Rev. E*, 2004, **70**, 051805.

49. S. D. Kelman, B. W. Rowe, C. W. Bielawski, S. J. Pas, A. J. Hill, D. R. Paul and B.D. Freeman, *J. Membr. Sci.*, 2008, **320**, 123.

50. H. A. Lorentz, *The Theory of Electrons*, Dover Publications, Inc., New York, 1952.

51. D. W. V. Krevelen, *Properties of Polymers*, Elsevier, Amsterdam, 1990.

52. Y. Ichiraku, S. A. Stern and T. Nakagawa, *J. Membr. Sci.*, 1987, **34**, 5.

53. K. Nagai, B. D. Freeman and A. J. Hill, *J. Polym. Sci. Part B: Polym. Phys.*, 2000, **38**, 1222.

54. D. Cangialosi, H. Schut, A. van Veen and S. J. Picken, *Macromolecules*, 2003, **36**, 142.
55. G. Dlubek, D. Kilburn and M. A. Alam, *Macromol. Symp.*, 2004, **210**, 11.
56. P. E. Mallon, in *Positron & Positronium Chemistry*, ed. Y. C. Jean, P. E. Mallon and D. M. Schrader, World Scientific, New Jersey, 2003, pp. 253–280.
57. S. J. Tao, *J. Chem Phys.*, 1972, **56**, 5499.
58. M. Eldrup, D. Lightbody and J. N. Sherwood, *Chem. Phys.*, 1981, **63**, 51.
59. R. Suzuki *et al.*, *Jpn. J. Appl. Phys., Part 2*, 1991, **30**, L532.
60. J. Algers, R. Suzuki, T. Ohdaira and F. H. J. Maurer, *Polymer*, 2004, **45**, 4533.
61. S.-H. Huang, W. S. Hung, D. J. Liaw, C. L. Li, S. T. Kao, D. M. Wang, M. D. Guzman, C. C. Hu, Y. C. Jean, K. R. Lee and J. Y. Lai, *Macromolecules*, 2008, **41**, 6438.
62. S.-H. Huang, W. S. Hung, D. J. Liaw, H. A. Tsai, G. J. Jiang, K. R. Lee and J. Y. Lai, *Polymer*, 2010, **51**, 1370.
63. W.-S. Hung, M. De Guzman, S.-H. Huang, K.-R. Lee, Y. C. Jean and J.-Y. Lai, *Macromolecules*, 2010, **43**, 6127.
64. B. W. Rowe, B.D. Freeman and D.R. Paul, *Polymer*, 2009, **50**, 6149.
65. J. Algers, P. Sperr, W. Egger, G. Kögel and F. H. J. Maurer, *Phys. Rev. B*, 2003, **67**, 125404(1).
66. A. Serghei, H. Huth, C. Schick and F. Kremer, *Macromolecules*, 2008, **41**, 3636.
67. C. J. Ellison and J. M. Torkelson, *J. Polym. Sci. Part B: Polym. Phys.*, 2002, **40**, 2745.
68. C. L. Soles, J. F. Douglas, W.-l. Wu, H. Peng and D. W. Gidley, *Macromolecules*, 2004, **37**, 2890.
69. C. M. Agrawal, K. J. Heater and A. J. Hill, *J. Mater. Sci. Lett.*, 1989, **V8**, 1414.
70. A. J. Kovacs and J. M. Hutchinson, *J. Polym. Sci. Polym. Phys. Ed.*, 1979, **17**, 2031.
71. J. Hadac, *et al.*, *J. Non-Cryst. Solids*, 2007, **353**, 2681.
72. D. Cangialosi *et al.*, *Phys. Rev. B: Condens. Matter,* 2004, **70**, 224213(1).
73. D. J. Enscore, H. B. Hopfenberg, V. T. Stannett and A. R. Berens, *Polymer*, 1977, **18**, 1105.
74. A. H. Chan and D. R. Paul, *J. Appl. Polym. Sci.*, 1980, **25**, 971.
75. G. K. Fleming and W. J. Koros, *Macromolecules*, 1990, **23**, 1353.
76. S. M. Jordan, W. J. Koros and G. K. Fleming, *J. Membr. Sci.*, 1987, **30**, 191.
77. B. W. Rowe, B. D. Freeman and D. R. Paul, *Polymer*, 2010, **51**, 3784.
78. J. H. Kim, W. J. Koros and D. R. Paul, *J. Membr. Sci.*, 2006, **282**, 21.
79. J. H. Kim, W. J. Koros and D. R. Paul, *J. Membr. Sci.*, 2006, **282**, 32.
80. C. A. Scholes, G. Q. Chen, G. W. Stevens and S. E. Kentish, *J. Membr. Sci.*, 2010, **346**, 208.
81. M. Wessling, M. Lidon Lopez and H. Strathmann, *Sep. Purif. Technol.*, 2001, **24**, 223.

82. N. R. Horn and D. R. Paul, *Polymer*, 2011, **52**, 1619.

83. A. Q. Tool, *J. Res. Natl. Bur. Stand.*, (*U. S.*), 1945, **34**, 199.

84. A. J. Kovacs, J. M. Hutchinson and J. J. Aklonis, in *The Structure of Non-Crystalline Materials*, ed. P. H. Gaskell, Taylor and Francis, London, 1977, pp. 153–163.

85. R. W. Rendell, K. L. Ngai and D. J. Plazek, *J. Non-Cryst. Solids,* 1991, **131–133**, 442.

86. J. G. Curro, R. R. Lagasse and R. Simha, *Macromolecules*, 1982, **15**, 1621.

87. A. W. Thornton, K. M. Nairn, A. J. Hill, J. M. Hill and Y. Huang, *J. Membr. Sci.*, 2009, **338**, 38.

88. M. S. McCaig, D. R. Paul and J. W. Barlow, *Polymer*, 2000, **41**, 639.

89. J. Y. Park and D. R. Paul, *J. Membr. Sci.*, 1997, **125**, 23.

90. J. H. Kim, J. Jang and W. C. Zin, *Langmuir*, 2000, **16**, 4064.

91. L. Starannikova, V. Khodzhaeva and Y. Yampolskii, *J. Membr. Sci.*, 2004, **244**, 183.

92. P. M. Budd, N. B. McKeown, B. S. Ghanem, K. J. Msayib, D. Fritsch, L. Starannikova, N. Belov, O. Sanfirova, Y. Yampolskii and V. Shantarovich, *J. Membr. Sci.*, 2008, **325**, 851.

93. H. B. Park, C. H. Jung, Y. M. Lee, A. J. Hill, S. J. Pas, S. T. Mudie, E. Van Wagner, B. D. Freeman and D. J. Cookson, *Science*, 2007, **318**, 254.

94. A. J. Hill, S. J. Pas, T. J. Bastow, M. I. Burgar, K. Nagai, L. G. Toy and B. D. Freeman., *J. Membr. Sci.*, 2004, **243**, 37.